JAPANESE JOURNAL OF APPLIED PHYSICS
VOL. 26, NO. 5, MAY, 1987, pp. 649-654

Component Assignments of the Raman Spectrum from Highly Elongated Silica Glass Filbers

Kazuhiro EMA, Yoshinori HIBINO,† Hidemi SHIGEKAWA and Shin-ichi HYODO

Department of Applied Physics, the University of Tokyo, Bunkyo-ku, Tokyo 113
†*NTT Electrical Communications Laboratories, Tokai, Ibaraki 319-11*

(Received December 27, 1986; accepted for publication February 21, 1987)

Raman spectra from glass fibers subjected to high tensile stresses (up to 4 GPa) were decomposed into their Gaussian components, which were then assigned to normal vibrational modes of either SiO_4 or Si_2O molecules using an "isolated molecule" model. Such molecule-related parameters as force constants, Raman coupling constants and the dispersion of the intertetrahedral bond angle were estimated from the frequencies, heights and widths of the components. It is concluded from the analysis that the Raman spectrum change associated with the application of tensile stress arises principally, not from a Si-O bond stretching or Si-O-Si bond angle broadening, but from a change in the tetrahedral angles of the SiO_4 molecules constituting silica glass networks.

§1. Introduction

Pure silica glass exhibits six peaks in its first-order Raman spectra: a dominant peak at 440 cm^{-1} (usually assigned to bond-bending vibrations), there small peaks at 800, 1065 and 1200 cm^{-1} (usually assigned to bond-stretching vibrations), and two sharp peaks at 495 and 604 cm^{-1} (assigned to "planar rings" by Galeener *et al.*[1,2]). These peak assignements to vibrational modes, however, are not so convincing in the case of silica glass as in that of crystalline silica, since in the former case the peaks are inevitably blunted from the lack of long-range lattice periodicity.

To interpret the Raman spectra of silica glass, Sen *et al.*[3,4] proposed an "NN-CF-ICRN" model (wherein are taken into consideration only nearest-neighbor central-force interactions among the tetrahedrons forming continuous random networks). Using this model they expressed Raman peak frequencies as functions of intertetrahedral angles, atomic masses and central forces. With regard to the Raman peak shifts caused by the isotope substitution of glass constituents and to an associated change in the fictive temperature of glasses, a good agreement was reported between their calculation and experiments.[5-7]

Walrafen *et al.*[8] and Hibino *et al.*[9] observed that the shape of the 440 cm^{-1} peak was susceptible to tensile stresses applied to silica glass fibers. Since the NN-CF-ICRN model provides no information about changes in the Raman intensity, they decomposed the observed Raman spectra into Gaussian components in order to interpret the stress effect more or less quantitatively.[9,10] However, they failed to assign the Gaussian components to the vibrational modes of SiO_2 networks. The purpose of this communication is to achieve those component assignments, and to show that the stress effect can successfully be interpreted if the reduced Raman spectra are decomposed into seven main Gaussian components representing the normal vibrational modes of either SiO_4 tetrahedral or Si_2O triangular molecules.

§2. Spectrum Decomposition into Normal Modes

According to Shuker and Gamon,[11] the Raman scattering intensity (Stokes shift at a frequency ω) for amorphous solids is given by

$$I(\omega)=\sum_b C_b\cdot[1+n(\omega)]\cdot g_b(\omega)/\omega, \tag{1}$$

where b denotes a vibration mode and $n(\omega)$ a Bose function, while $g_b(\omega)$ and C_b represent the density of states and the Raman coupling constant corresponding to the mode b, respectively. (In deriving eq. (1), C_b is assumed to be independent of ω.) From eq. (1) one can readily write the reduced Raman intensity $I^\gamma(\omega)$ as

$$I^\gamma(\omega)=I(\omega)\cdot\omega/[1+n(\omega)]=\sum_b C_b\cdot g_b(\omega), \tag{2}$$

i.e. $I^\gamma(\omega)$ becomes a linear function of the density of states.

In deriving eq. (1) Shuker and Gamon replaced a δ function (that was employed in the case of crystalline silica) with $g_b(\omega)$, assuming that a breakdown of momentum selection rule (i.e. dispersion in Raman frequencies) should result from such a mechanical disorder as that exemplified by a variation in bond length or bond angle. In the present treatment we further assume that this disorder can be expressed in terms of a Gaussian distribution function if it distributes uniformly in a silica glass structure, i.e., if there are no structural polarization or orientation effects. Using this assumption we decomposed the observed $I^\gamma(\omega)$ into the Gaussian components so that they might represent the density of each state. Typical results are summarized in Fig. 1, where the solid line indicates the reduced intensity observed for a silica glass fiber and the dashed lines indicate the results of a decomposition, which was carried out as follows.

First, attention was focussed on the normal vibration modes of a tetrahedral (AX_4 type) and a triangular (A_2X type) molecule. As is schematically illustrated in Fig. 2, the AX_4 type has four normal modes, i.e., a non-degenerate scalar A_1 (V1), a doubly degenerate tensor E

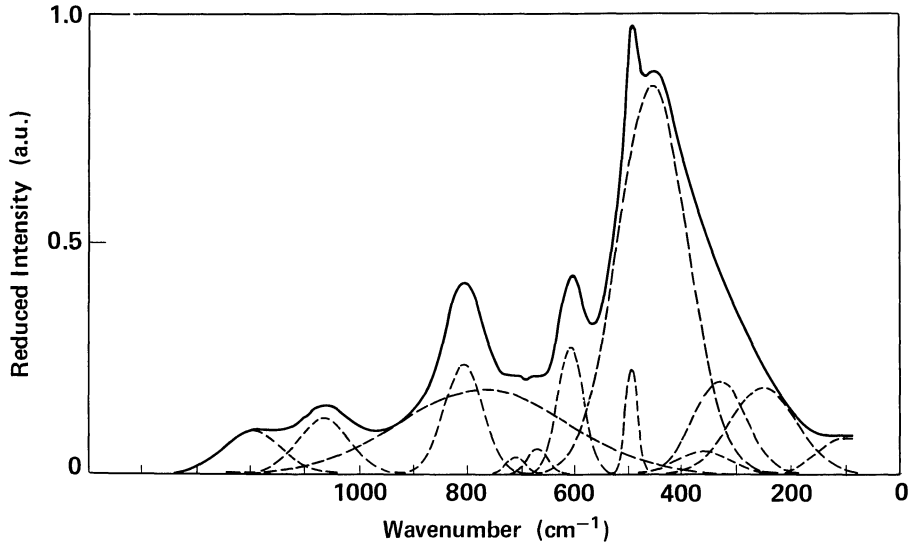

Fig. 1. Gaussian components of a reduced Raman spectrum observed for a silica glass fiber. The dashed lines indicate the components estimated while the solid line indicates the observed reduced spectrum.

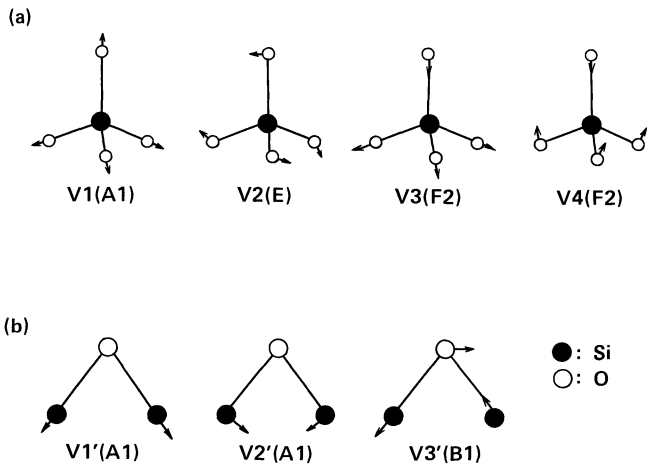

Fig. 2. Normal vibration modes of a tetrahedral molecule (a) and a triangular molecule (b).

Table I. Parameters determined by decomposing the Raman spectrum obtained from silica glass fibers.

Assignment	Center	Width	Height	Area(%)	C_b
/	100	40	50	2.6	/
V2	250	50	120	7.8	0.35
V'2	330	40	130	6.8	0.53
/	360	40	30	1.6	/
V4	455	55	550	39.6	2.63
planar-ring	495	9	150	1.7	16.5
planar-ring	608	20	180	4.7	2.82
/	670	15	35	0.7	/
/	710	15	25	0.5	/
V'1	770	130	120	20.4	2.20
V1	808	30	155	6.1	1.00
V3	1065	40	75	3.9	0.47
V'3	1195	45	60	3.5	0.33

C_b: Raman coupling constant

(V2) and two triply degernerate vector F_2 (V3, V4) modes. On the other hand, the A_2X type has three, i.e., two non-degenerate scalar A_1 (V'1, V'2), and a non-degenerate antisymmetric B (V'3) mode. Bearing these vibration modes in mind and assuming* that there are no interactions between the triangular and tetrahedral modes of vibration, we determined their frequencies regarding the SiO_4 and Si_2O molecules using the several data known for molecules with a similar structure (SiF_4, SiO_2, F_2O, etc.).

The next step was to determine a set of seven Gaussian components which have center frequencies approximately equal to one of the above-stated vibration frequencies. With the aid of a personal computer the height and width of each component were varied in a successive manner so that the superposition of all the components might agree with the observed reduced intensity $I(\omega)$. However, a satisfying conformation, say with an error below 1%, could not be achieved without introducing six subsidiary components. Their assignments are listed in Table I, where the two components at 495 and 604 cm^{-1} are regarded as planar-ring-related peaks while the other four are considered to be components merely for a compensation of the seven normal modes.

The Gaussian components thus determined appear to represent very well the normal vibration modes (shown in Fig. 1) for silica glass. Hence, in the succeeding step we tried to express their frequencies in terms of molecule-related parameters, such as the interatomic force constants, atomic masses and bond angles. For this purpose the GF matrix method was used.[11-13] As is illustrated in Fig. 3, the F matrix used had diagonal and non-diagonal components corresponding to the force and interaction constants, respectively. For the sake of simple calculations we neglected interactions between the bond-stretching and bond-bending vibrations. We also assumed that all of the Si-O bond length (r_0), the O-Si-O bond angle (ϕ_0) and the Si-O-Si bond angle (θ_0) were constants. To determine the eigenvalues of the GF matrix, we successively repeated a unitary conversion. As a result, the frequencies of the seven Gaussian components could be written as follows:

$$\omega_1^2(808\ \mathrm{cm}^{-1}) = (f_1 + 3f_3)(1/m_0 + [1 + 3\cos\phi_0]/m_{si}), \quad (3)$$

*This does not rigorously hold for an actual glass network.

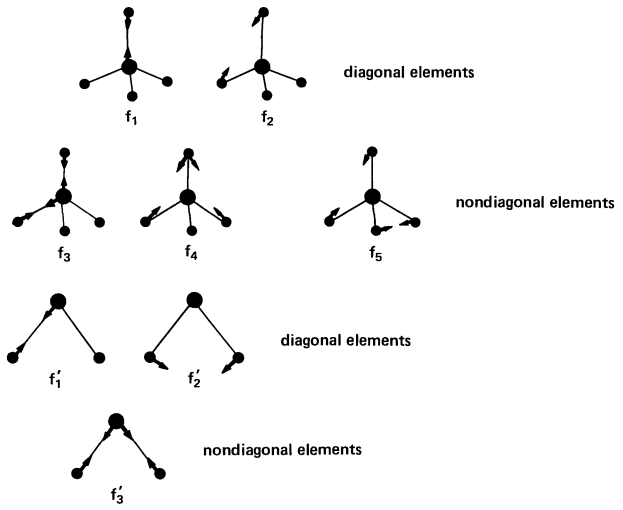

Fig. 3. F matrix elements of tetrahedral and triangular molecules; the elements have both diagonal and non-diagonal components corresponding to force and interaction constants, respectively.

$$\omega_2^2(250\ \mathrm{cm}^{-1})=2(f_2+f_5-2f_4)(1+\cos\phi_0)^{-1}/m_0, \quad (4)$$

$$\omega_3^2(1065\ \mathrm{cm}^{-1})=(f_1-f_3)(1/m_0+[1-\cos\phi_0]/m_{si}), \quad (5)$$

$$\omega_4^2(455\ \mathrm{cm}^{-1})=2(f_2-f_5)(1/m_0+[1-\cos\phi_0]\times\tan^2(\phi_0/2)/m_{si}), \quad (6)$$

$$\omega_1'^2(770\ \mathrm{cm}^{-1})=(f_1'+f_3')([1+\cos\theta_0]/m_0+1/m_{si}), \quad (7)$$

$$\omega_2'^2(330\ \mathrm{cm}^{-1})=2f_2'([1-\cos\theta_0]/m_0+1/m_{si}), \quad (8)$$

and

$$\omega_3'^2(1195\ \mathrm{cm}^{-1})=(f_1'-f_3')([1-\cos\theta_0]/m_0+1/m_{si}). \quad (9)$$

In the above m_b and m_{si} denote the mass of an oxygen and that of a slicon atom, respectively. The central frequency of each component is indicated as a wavenumber in its respective parentheses.

Among published X-ray diffraction data we chose 1.61 Å and 144° as the average value of r_0 and of θ_0, respectively. On the other hand, ϕ_0 was estimated to be 109.5° (i.e., $\cos\phi_0=-1/3$) from a geometrical requirement for a tetrahedron. A comparison of both sides of eqs. (3) to (9) (into the right-hand side of which the above values were substituted) yielded the following F matrix elements:*

$$f_1=6.1,\quad f_2=0.29,\quad f_3=0.02,\quad f_4=-0.03,$$
$$f_5=-0.16,\quad f_1'=6.5,\quad f_2'=0.22,\quad f_3'=0.81$$
$$[\mathrm{mdyn/Å}]. \quad (10)$$

One should note in eq. (10) that the value of f_1 is very close to that of f_1'. This suggests the validity of the present analysis; since both of them represent the stretching force constant for a Si-O bond, there is no reason why they should differ so much, though f_1 is concerned with the bonds constituting a tetrahedron while f_1' with those constituting a triangle. That f_2 and f_2' are nearly equal is also noteworthy, since this indicates that the (bond-bending) force constant for the angle O-Si-O is nearly equal to that for Si-O-Si.

In evaluating the F matrix elements we assumed that all or r_0, ϕ_0 and θ_0 were always constant throughout a glass network. Actually, however, these values must more or less scatter. This is considered to be the cause of the frequency widths of the observed Gaussian components.

The fluctuation range of θ_0 could be estimated from the width of the V'1, V'2 and V'3 components using eqs. (7) to (9). The solid lines in Fig. 4 indicate the dependence of the Si-O-Si bond angle (θ_0) on the wave number; to obtain this relation, we assumed that the vibrations were harmonic and that none of f_1', f_2' and f_3' were affected by a small change in θ_0. The horizontal

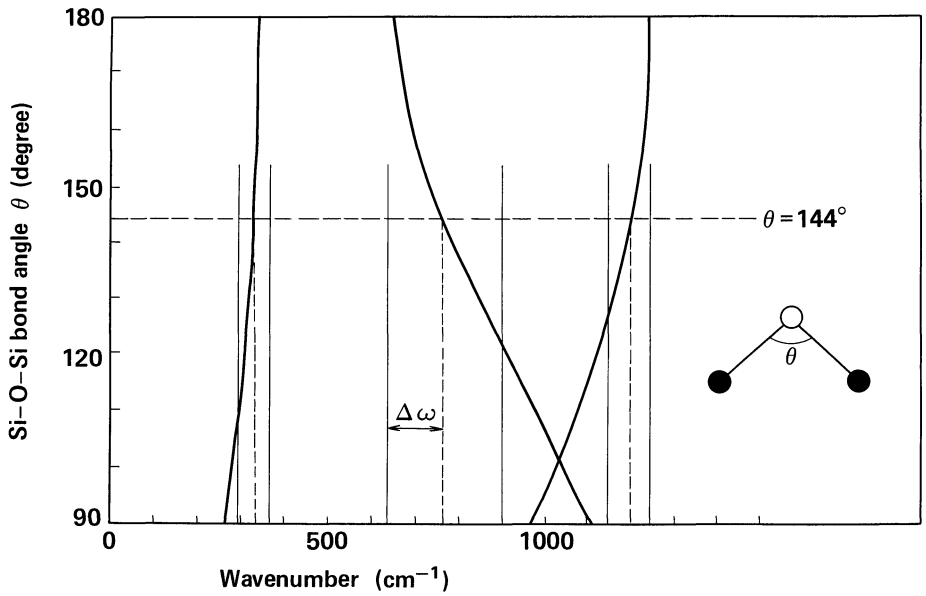

Fig. 4. The Si-O-Si bond angle as a function of the vibration wavenumber. The abscisae of the intersections between the horizontal dashed line and the solid lines indicate the center-of-component frequencies. The width between the intersections and the vertical solid lines, such as $\Delta\omega$ shown, represent the extent of frequency fluctuation (the values of $\Delta\omega$, the width of Gaussian components, are summarized in Table I).

*To determine the values of f_4 and f_5 in eq. (10) we used $f_2+f_5+4f_4=0$, a relation resulting from a unitary conversion.

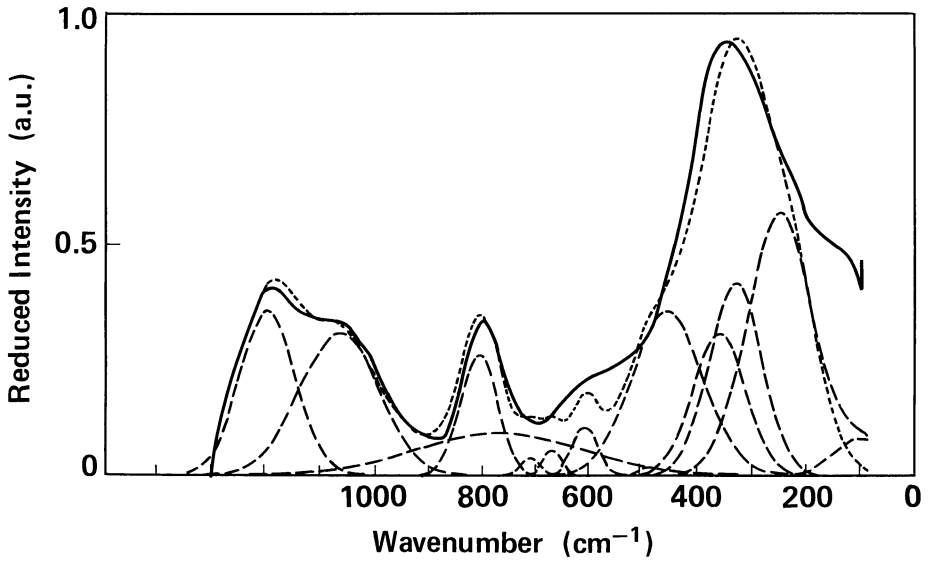

Fig. 5. Gaussian components (the dashed lines) adjusted to conform with the neutron diffraction spectrum (the solid line) observed by Leadbetter and Stringfellow. The dotted line indicates the spectrum synthesized from all the components.

dashed line in Fig. 4 shows the average of θ_0 (144°), whereas the abscissae of the intersections between the dashed and the solid lines correspond to the center-of-component frequencies. The vertical dashed lines represent the extent of frequency fluctuations ($\Delta\omega$) by their deviation in abscissae from their respective center-of-component frequencies. Using this relation and the data on $\Delta\omega$ (summarized in Table I), we can conclude that the Si-O-Si bond angle in silica glass fibers lies in a range $120° < \theta_0 < 180°$, in good agreement with the results from X-ray diffraction studies.

As can be seem in eq. (2), the reduced Raman spectra are a linear function of the density of state $g_b(\omega)$. However, the spectra do not represent the summation of all $g_b(\omega)$'s, since the Raman coupling constant C_b may differ from mode to mode. In order to estimate C_b for different normal modes of vibration, we employed neutron diffraction data provided by Leadbetter and Stringfellow:[14] We adjusted the heights of our previously decomposed spectra (without changing their center frequencies and frequency widths) so that the spectrum synthesized from the decomposed spectra (the dotted line in Fig. 5) might conform to that of neutron diffraction (the solid line). The last column of Table 1 shows the relative magnitudes of C_b, thus determined. These results seem to suggest that, aside from some of the planar-ring-related modes, either the tetrahedral V4 or the triangle V′1 mode is most likely to undergo Raman coupling.

§3. Tensile stress effects on Raman Spectra

Figure 6(a) shows the reduced intensity spectra obtained from the silica glass fibers which were either unstrained or strained. It can be seen that under a stress of 4 GPa the dominant peak at 440 cm^{-1} was decreased in height by 18% and was slightly broadened from that observed for a stress-free fiber. By means of a deconvolution of these spectra into Gaussian components (similar to the present study) it was shown that, as is illustrated in Fig. 6(b), the tensile stress affects no other components than that corresponding to the tetrahedral V4 mode. This

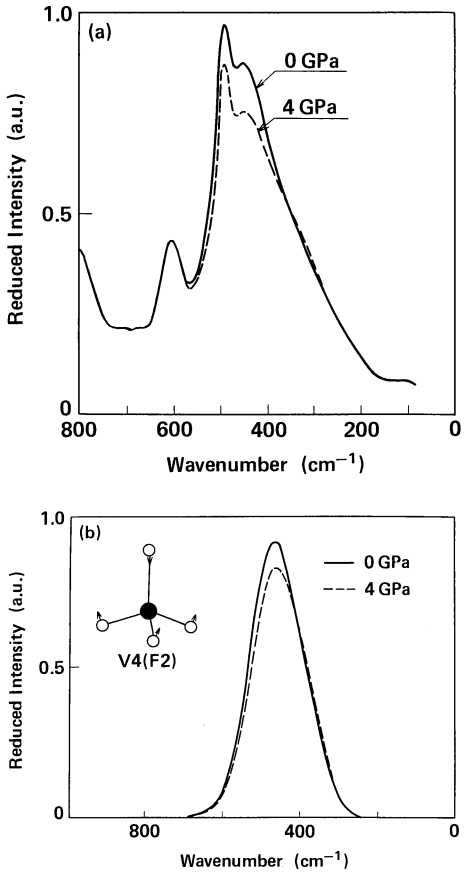

Fig. 6. (a) Reduced intensity spectra for a silica glass fiber which was either free of stress or under 4 GPa tensile stress. (b) The change of a Gaussian component corresponding to the tetrahedral V4 mode under 4 GPa tensile stress, which is consistent with the change shown in (a).

change in the V4 mode spectrum is now discussed in connection with the glass network structure.

We can naturally presume that a tensile stress causes an elongation in the Si-O bonds, an increase in the Si-O-Si bond angles and a distortion of SiO_4 tetrahedrons. The effect of Si-O bond elongation on the Raman spectrum is hardly possible to estimate from eqs. (3) to (9), since they

do not include r_0. However, the stress-induced change in r_0 must be negligible in comparison with that in bond angles, since the bond-stretching force constants (f_1 and f_1' in eq. (10)) are much greater than the bond-bending ones (f_2 and f_2'). Hence, in view of eq. (6)—the expression for the V4 mode frequency—that depends solely on ϕ_0, it is apparent that a stress-induced change in ϕ_0, i.e., the distortion of a SiO_4 tetrahedron, must play a significant role in the spectrum behavior of the V4 mode.

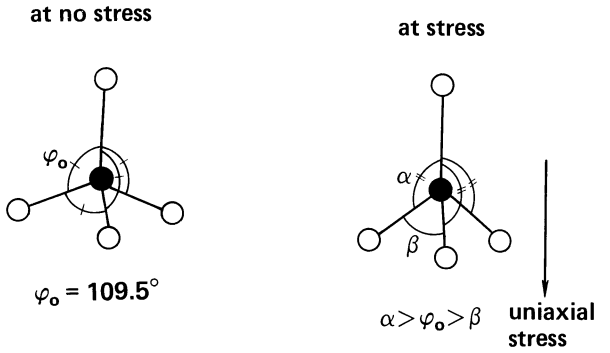

Fig. 7. Schematic illustration for the distortion of a tetrahedral molecule under uniaxial stress.

If the O-Si-O bond angles α and β, are defined in the manner shown in Fig. 7, they must have the relation

$$3\cos^2\alpha + 4\cos\beta + 1 = 0, \tag{11}$$

where

$$(\alpha > \phi_0 = 109.5^\circ \text{ and } \beta < \phi_0 = 109.5^\circ).$$

Using this relation, we calculated the dependence of each normal mode frequency of a SiO_4 tetrahedron on α. The results are shown in Fig. 8, where the dashed line indicates $\phi_0(=109.5^\circ)$, the bond angle of undistorted tetrahedrons. One can see in Fig. 8 that two triply degenerate F_2 modes (V3 and V4) become clearly decoupled into a non-degenerate (A_1) and a doubly degenerate (E) mode with an increase in the deviation of α from ϕ_0. Hence, it seems very plausible that, as illustrated in Fig. 9, the tensile stress will cause a shift in the frequencues of the E and A_1 modes and, thus, to change the superposition of these two modes, i.e., the V4 mode. Figure 9 seems to also explain the reason for the stress-induced lowering and blunting of the V4 mode component.

The V4 mode component was also found to decrease in area as a result of the tensile stress. This can be ascribed

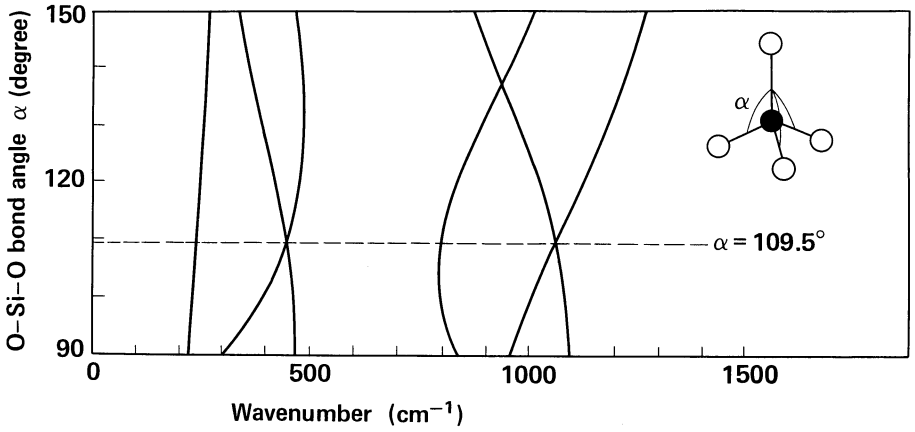

Fig. 8. Wavenumber of normal mode vibrations for a SiO_4 tetrahedron as a function of α.

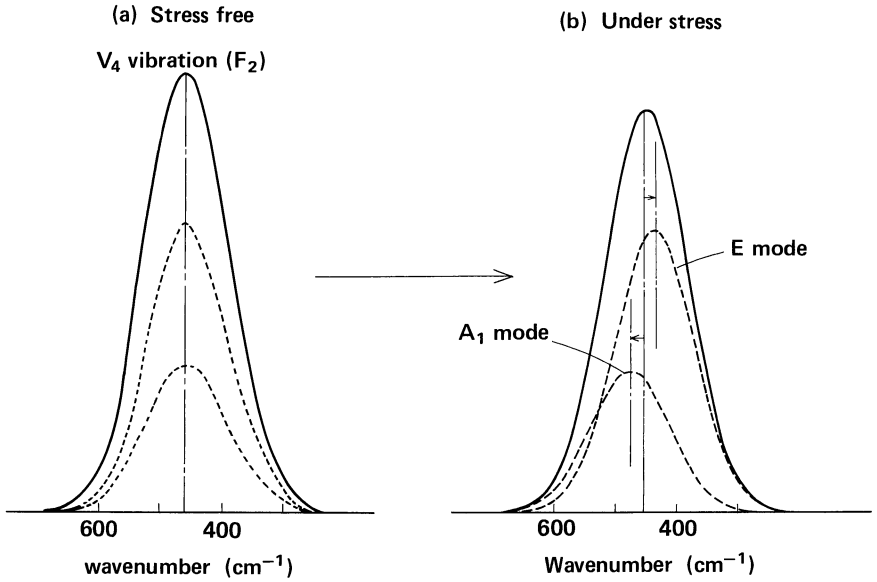

Fig. 9. Reduced intensity change associated with the stress-caused decoupling of the V4 vibration (triply degenerate F_2 mode) into a non-degenerate A_1 and a doubly degenerate E mode.

to a decrease in the Raman coupling constant C_b: Though it is largest for the V4 mode among the normal vibration modes (Table I), it should be lessened with the growth of asymmetry of SiO_4 tetrahrdrons. Since the Si-O-Si bond angle α is estimated to vary from ϕ_0 ($=109.5^\circ$ at zero stress) to 115° (at 4 GPa), the tetrahedron can be elongated by 6.7% along the tensile axis—close to 6.5%, the measured strain of sample fibers.

In our previous study, no tensile-stress effects were observed regarding the Gaussian components assigned to Si-O-Si triangle modes. However, Fig. 4 indicates that the frequency of the V′1 and the V′2 mode will be raised, while that of the V′3 mode will be lowered, with increasing θ ($=144^\circ$). This indicates that the average of θ is scarcely affected by tensile stresses, through θ for each triangle in a glass nework may increase or decrease depending on the direction of the Si-Si bond of the triangle concerned, *e.g.*, on whether the direction is parallel or orthogonal to stress axis. If this actually occurs, an extention of the fluctuation range of θ must result in the broadening of the spectra concerned, which seem, however, to have been too small for us to detect the effects.

Stress effects were also not observed for the 495 and 604 cm^{-1} peaks, which are usually ascribed to the presence of "planar rings", i.e., the defects with a regular ring-like form. This suggests that planar rings are less susceptible to external strain than their surrounding amorphous network.

§4. Discussion

To realize the advantage of the isolated molecule model adopted in the present study over the NN-CF-ICRN model stated in §1, one should compare eqs. (3) to (9) with the corresponding expressions based on the NN-CF-ICRN model. According to Sen *et al.*, they are written as

$$\omega_{1n}^2=(\zeta/m_0)(1+\cos\theta), \tag{12}$$

$$\omega_{2n}^2=(\zeta/m_0)(1-\cos\theta), \tag{13}$$

$$\omega_{3n}^2=(\zeta/m_0)(1+\cos\theta)+(4\zeta/3m_{si}), \tag{14}$$

and

$$\omega_{4n}^2=(\zeta/m_0)(1-\cos\theta)+(4\zeta/3m_{si}). \tag{15}$$

In the above m_0 and m_{si} denote the mass of an oxygen and that of a silicon atom, respectively, while ζ is the central force due to the Born potential and θ the Si-O-Si bond angle. It should be noted that, although eqs. (12) to (15) represent the vibrations of a SiO_4 tetrahedron for both V1 and V3 mode, (bond-stretching) they do not include V2 and V4 modes since no forces other than central forces are considered in the NN-CF-ICRN model.

On the basis of these equations Sen *et al.* assigned four dominant Raman peaks of silica glass at 440, 800, 1065 and 1200 cm^{-1} to ω_{1n}, ω_{3n}, ω_{4n}(TO), and ω_{4n}(LO), respectively. According to Galeener *et al*,[5,6] a Raman frequency shift caused by the $Si^{28}\rightarrow Si^{30}$ and $O^{16}\rightarrow O^{18}$ isotope substitution in silica glass agreed with their prediction based on the NN-CF-ICRN model. However, they were unable to explain in terms of the NN-CF-ICRN model their observation on a slight shift in the dominant peak at 440 cm^{-1}, which also resulted from the $Si^{28}\rightarrow Si^{30}$ substitution. This is no wonder, since according to eq. (12) ω_{1n} has no connection with the atomic mass of Si. On the other hand, any of their results are easy to interpret from eqs. (3) to (9), i.e., in terms of our isolated molecule model.

Among the Raman spectrum components shown in Table I some, such as at 100, 360, 710 and 770 cm^{-1}, have been left unassigned. This is simply because the tensile stress effects on some of them were very slight, even under very high stresses. To make a complete assignment, an experimental study employing a much higher stress is necessary; such a study does not appear impossible because 4 GPa is still much lower than the theoretical strength of silica glass. It should be noted here than an effect similar to that of tensile stress on Raman spectra, i.e. the lowering and broadening of the dominant peak at 440 cm^{-1}, has been observed for silica glass fibers drawn at a very high speed* and also for glasses stabilized at 1000 and 1300°C.[15]

§5. Conclusion

Reduced Raman spectra from pure silica glass fibers were decomposed into Gaussian components, which were then assigned to the normal vibrational modes of a SiO_4 tetrahedron and of a Si_2O triangle on the basis of the isolated molecule model. This enabled us to make a plausible interpretation about the effect of tensile stress on the spectra and to conclude that the distortion of SiO_4 tetrahedrons in a glass network is primarily responsible for the effect.

In the light of the present study seven vibration modes seem to be more suited for the Raman spectrum representation of silica glass than the four vibration modes which on the basis of the NN-CF-ICRN model.

References

1) F. L. Galeener: Solid State Commun. **44** (1982) 1037.
2) F. L. Galeener, R. A. Barrio, E. Martinez and R. J. Elliott: Phys. Rev. Lett. **53** (1984) 2494.
3) P. N. Sen and M. F. Thorpe: Phys. Rev. B **15** (1977) 4030.
4) F. L. Galeener: Phys. Rev. B **19** (1979) 4292.
5) F. L. Galeener and J. C. Mikkelsen, Jr.: Phys. Rev. B **23** (1981) 5527.
6) F. L. Galeener and A. E. Geissberger: Phys. Rev. B **27** (1983) 6199.
7) A. E. Geissberger and F. L. Galeener: Phys. Rev. B **28** (1983) 3266.
8) G. E. Walrafen, P. N. Krishnan and S. W. Freiman: J. Appl. Phys. **52** (1981) 2832.
9) Y. Hibino, H. Hanafusa, K. Ema and S. Hyodo: Appl. Phys. Lett. **47** (1985) 812.
10) G. E. Walrafen and P. N. Krishnan: Appl. Opt. **21** (1982) 359.
11) R. Shuker and R. W. Gammon: Phys. Rev. Lett. **25** (1970) 222.
12) K. Nakamoto: *Infrared Spectra of Inorganic and Coordination Compounds* (John Wiley & Sons, Inc., New York, 1963).
13) N. B. Colthup, L. H. Daly and S. E. Wiberley: *Introduction to Infrared and Raman Spectroscopy* (Academic Press, New York and London, 1964).
14) A. J. Leadbetter and M. W. Stringfellow: *Neutron Inelastic Scattering, Proc. Grenoble Conf., 1972* (IAEA, Vienna, 1974) pp. 501-514.
15) S. W. Barber: *The Physics of SiO_2 and Its Interfaces, Proc. 1978* (Pergamon Press, New York, 1978) p. 139.

*This result will be reported in a separate paper.